UNIVERSIDADE DE SÃO PAULO

INSTITUTO DE FÍSICA
CAIXA POSTAL 20516
01498 - SÃO PAULO - SP
BRASIL

PUBLICAÇÕES

IFUSP/P-504

PHOTONEUTRON CROSS SECTIONS

by

E. Wolynec, V.A. Serrão, P. Gouffon, Y. Miyao and M.N. Martins

Instituto de Física, Universidade de São Paulo

Dezembro/1984

PHOTONEUTRON CROSS SECTIONS

E. WOLYNEC, V.A. SERRÃO, P. GOUFFON, Y. MIYAO

AND M.N. MARTINS

INSTITUTO DE FÍSICA DA UNIVERSIDADE DE

SÃO PAULO, SÃO PAULO, SP, BRAZIL

A B S T R A C T

The differences between the Saclay and Livermore photoneutron cross sections are discussed. It is shown that the differences between their (γ,n) and $(\gamma,2n)$ cross sections arise from the neutron multiplicity sorting. Measurements of the (e,n) and (e,2n) cross sections in ^{181}Ta show that Livermore has the correct multiplicity sorting.

1. INTRODUCTION

The giant dipole resonance has always been of central interest in photonuclear reaction studies, both theoretical and experimental. It corresponds to the fundamental frequency for absorption of electric dipole radiation by the nucleus as a whole.

Over the past three decades many studies of photonuclear reactions have been made, for many nuclei through the periodic table, in the attempt to delineate the systematics of photon absorption by nuclei in general and of the giant electric dipole resonance, which dominates the absorption process at energies between 10 and 30 MeV, in particular. The large effort that has been put into these studies is justified by the fact that the theory of the interaction of electromagnetic radiation with nuclei is perhaps the best understood in nuclear physics: if the interaction in the entrance channel is understood, then the effects of the purely nuclear forces can be studied directly by measuring either the photon absorption cross sections or the products of nuclear photodisintegration.

Most of the work in this area was carried out by two Laboratories, Saclay and Livermore, measuring photoneutron cross sections using monoenergetic photon beams. The combined studies of these two Laboratories span the whole periodic table, in a quite complete systematics of the E1 giant resonance. The use of monoenergetic photon beams has given rise to cross

section measurements with high resolution, and especially to an improved knowledge of the cross sections above the peak of the giant resonance. Higher-multiplicity cross sections have been measured directly and their systematics studied, and more accurate information on structure throughout the giant resonance obtained. The quality of the data produced has justified well the effort necessary to develop and utilize monoenergetic photon beams.

From those detailed studies many important properties of the E1 giant resonance have been obtained. There is, however, a serious conflict between the data from those Laboratories. There are systematic differences in the shapes and magnitudes of their (γ,n) and $(\gamma,2n)$ cross sections. Because of these differences, from the Saclay data it turns out that for heavy nuclei there is 15-20% of direct contribution in the reaction mechanism, while the Livermore data supports a dominant statistical decay of the E1 giant resonance.

In a recent comment[1], it was shown that the differences between the Saclay and Livermore photoneutron cross sections arise from differences in the neutron multiplicity sorting, that is, from the analysis that separates the measured neutron yields, $\sigma_{\gamma,Tn}$ ($\sigma_{\gamma,Tn} = \sigma_{\gamma,n} + 2\sigma_{\gamma,2n} + 3\sigma_{\gamma,3n} + \ldots$), in partial cross sections, $\sigma_{\gamma,in}$ ($i = 1, 2, \ldots$). The evidence presented in ref. 1 is insufficient to assess which Laboratory is performing the multiplicity sorting correctly. In order to adress this question we have measured the electrodisintegration of ^{181}Ta by neutron emission. The (e,2n) cross section is compared with

the cross sections predicted by the Saclay[2] and Livermore[3] data for this nucleus.

We will first discuss in detail the differences between the Saclay and Livermore data and the possible causes and consequences of these differences.

2. PHOTONEUTRON CROSS-SECTIONS

In Fig. 1 the (γ,Tn) cross sections measured by Saclay and Livermore for ^{181}Ta are shown. The experimental points are the Livermore data[3] and the line is a linear interpolation of the Saclay data[2]. $\sigma_{\gamma,Tn}$ is obtained from their published $\sigma_{\gamma,n}$ and $\sigma_{\gamma,2n}$ cross sections, which are available in digital form[4]. It is interesting to compare $\sigma_{\gamma,Tn}$ from both laboratories, because these are directly measured and the partial cross sections are obtained from the neutron multiplicity sorting. In Fig. 2 we show the ratio of these cross sections: $\sigma^S_{\gamma,Tn}/\sigma^L_{\gamma,Tn}$. The superscripts S and L refer to Saclay and Livermore, respectively. This ratio is reasonably constant. It has some structure which is caused by the fact that the energy scales of both measurements do not coincide exactly. As shown in Fig. 1 the position of the two peaks are slightly displaced. From all nuclei measured by Saclay and Livermore, discussed in ref. 1, ^{181}Ta is one of the few cases where we found such displacement in the energy scale. Since Saclay used their measurements to obtain the (γ,n)

and $(\gamma,2n)$ thresholds for ^{181}Ta and the obtained values are in good agreement with the calculated thresholds, we will assume their energy scale to be correct. In Fig.3 the ratio $\sigma^S_{\gamma,Tn}/\sigma^L_{\gamma,Tn}$ is shown, with the Livermore energy scale displaced by -410KeV. The solid lines in Fig. 2 and 3 result from the least squares fit of a constant to the ratio. The obtained constant for Fig. 3 is 1.22 ± 0.02. This constant reflects the difference between the absolute scales of Saclay and Livermore. In ref. 1 the values of the constants fitted to $\sigma^S_{\gamma,Tn}/\sigma^L_{\gamma,Tn}$ are given for each nucleus.

In Fig. 4 we show again $\sigma^S_{\gamma,Tn}$ and $\sigma^L_{\gamma,Tn}$, but with the Livermore data displaced by -410 KeV and multiplied by 1.22 in order to show both cross sections in the same energy scale and in the same absolute scale. The agreement between both measurements is excellent. In Figs. 5 and 6, that will be discussed subsequently, the Livermore data is displaced by -410 KeV and multiplied by 1.22.

In Figs. 5 and 6 we show, respectively, the (γ,n) and $(\gamma,2n)$ cross sections from Saclay and Livermore. Both (γ,n) cross sections are in good agreement up to the $(\gamma,2n)$ threshold. Above this energy there is an important difference: the Livermore cross section vanishes a few MeV above the $(\gamma,2n)$ threshold, in good agreement with the predictions of the statistical model, while the Saclay cross section presents a tail. In ref. 2 the observed tail of the Saclay cross section is interpreted as arising from fast neutrons that would have escaped detection in the Liver-

more measurement, leading to the conclusion that for ^{181}Ta the contribution of the "direct effect" in the photoneutron cross section is $n_d = 22 \pm 2\%$. As shown in Fig. 3, both Laboratories are detecting the same number of neutrons for all photon energies. If there were fast neutrons escaping detection in the Livermore measurement above 14 MeV, the ratio shown in Fig. 3 (or 2) should increase above this energy. Since both Laboratories agree as to the total number of neutrons detected it is clear that the differences in their (γ,n) and $(\gamma,2n)$ cross sections arise from the separation of the total counts into (γ,n) and $(\gamma,2n)$ events.

If we assume that the excess (γ,n) cross section in the Saclay measurement is caused by interpreting $(\gamma,2n)$ events as two (γ,n) events, that is, if we compute:

$$\sigma^{S*}_{\gamma,2n} = \sigma^{S}_{\gamma,2n} + \frac{1}{2}\,(\sigma^{S}_{\gamma,n} - 1.22\,\sigma^{L}_{\gamma,n}) \qquad (1)$$

we obtain for $\sigma^{S*}_{\gamma,2n}$ the solid line shown in Fig. 7. The modified $\sigma_{\gamma,2n}$ cross section from Saclay is now in excellent agreement with the $(\gamma,2n)$ cross section from Livermore (data points).

In order to show that the above conclusions do not depend on the displacement of the Livermore energy scale, in Figs. 8 and 9 we show, respectively, the Saclay and Livermore (γ,n) and $(\gamma,2n)$ cross sections without the displacement of the energy scale, but in the same absolute scale, and in Fig. 10 we show the modified Saclay cross section. The displacement of the energy

scale does not change the conclusions, only improves the agreement between the cross sections from Saclay and Livermore. The displacement of -410 KeV in the Livermore energy scale was chosen as the displacement that yielded the best χ^2 for the least squares fit of a constant to the ratio $\sigma^{S}_{\gamma,Tn}/\sigma^{L}_{\gamma,Tn}$.

As discussed in ref. 1, for all nuclei that were measured by both laboratories the same pattern was found:

a) Both laboratories are detecting the same number of neutrons versus the incident photon energy, apart from a constant, $R = \sigma^{S}_{\gamma,Tn}/\sigma^{L}_{\gamma,Tn}$, which reflects the difference between their absolute scales.

b) $\sigma^{S}_{\gamma,n}$ is bigger than $R\sigma^{L}_{\gamma,n}$ above the $(\gamma,2n)$ threshold.

c) $\sigma^{S}_{\gamma,2n}$ is smaller than $R\sigma^{L}_{\gamma,2n}$.

d) If $\sigma^{S}_{\gamma,2n}$ is modified using:

$$\sigma^{S*}_{\gamma,2n} = \sigma^{S}_{\gamma,2n} + \frac{1}{2}\,(\sigma^{S}_{\gamma,n} - R\sigma^{L}_{\gamma,n})$$

then $\sigma^{S*}_{\gamma,2n}$ and $\sigma^{S*}_{\gamma,n}$ are in good agreement with $\sigma^{L}_{\gamma,2n}$ and $\sigma^{L}_{\gamma,n}$, where $\sigma^{S*}_{\gamma,n} = \sigma^{S}_{\gamma,Tn} - 2\sigma^{S*}_{\gamma,2n}$.

In conclusion, the differences between the shapes and magnitudes of the Saclay and Livermore (γ,n) and $(\gamma,2n)$ cross sections are caused by the difference in the analysis that separates the total counts into (γ,n) and $(\gamma,2n)$ events.

In order to distinguish a $(\gamma,2n)$ event from two (γ,n)

events, highly efficient 4π neutron detectors are needed (since the efficiency for detecting two neutrons is the square of that for one). Both Saclay and Livermore use a slowing down type of detector, in which the neutrons produced during the short beam burst of a pulsed accelerator are moderated before being detected between beam bursts. Livermore uses a large array of $^{10}BF_3$ tubes, diposed in concentric rings, embedded in a paraffin or polyethylene matrix, and Saclay uses a large liquid scintillator. In order to be able to measure absolute cross sections and to differentiate between a $(\gamma,2n)$ event and two (γ,n) events, the detector efficiency must be known rather precisely.

The Livermore group has developed the ring-ratio technique for measuring the average neutron energy[5], based on the fact that the ratio of the counting rate in the outer ring of $^{10}BF_3$ detectors to that in the inner ring is a strong, monotonically increasing function of the energy of the photoneutrons. With the aid of calibrated neutron sources the efficiency is determined as a function of the neutron energy. Thus for every data run the average neutron energies for the (γ,xn) events are determined separately using the ring ratio measurements[5]. This enables the partial cross sections to be obtained using detector efficiencies appropriate to each photoneutron multiplicity, improving the accuracy of the branching ratios.

The large Gd-loaded liquid scintillator used by Saclay was calibrated only by means of a ^{252}Cf source. A calculated efficiency is used to justify a constant value for the

efficiency used in the photoneutron multiplicity sorting, on the basis that serious discrepancies arise only above neutron energies $E_n \cong 5$ MeV, whereas the energy of most photoneutrons does not exceed ~ 3 MeV[6]. Furthermore, eventhough the efficiency ε measured with the ^{252}Cf source is very close to one, the system is usually operated under timing conditions that reduce ε to ~ 0.6[2].

The overall detector efficiencies over the range of neutron energies important for giant resonance measurements are rather well known (to $\lesssim 3\%$)[5], so that the differences in the absolute scales of both Laboratories are primarily caused by uncertainty in the photon flux measurements. However, the branching between the various partial cross sections depends critically upon the efficiencies used, since for the (γ,xn) cross section the efficiency enters as ε^x. Thus, the fact that both laboratories agree, for all nuclei measured, as to the total number of emitted neutrons, apart from a constant factor due to differences in their absolute scales, but obtain different partial cross sections, could be explained by an error in the efficiency used by one of them.

3. ELECTRO AND PHOTODISINTEGRATION CROSS SECTIONS

The electrodisintegration cross section $\sigma_{e,x}(E_o)$ may be obtained from the photonuclear cross section $\sigma^{\lambda L}_{\gamma,x}(E)$

through an integral over the virtual photon intensity spectrum $N^{\lambda L}(E_o,E,Z)$[7]:

$$\sigma_{e,x}(E_o) = \int_o^{E_o-m} \sum_{\lambda L} \sigma_{\gamma,x}^{\lambda L}(E)\, N^{\lambda L}(E_o,E,Z)\, \frac{dE}{E} \qquad (2)$$

In Eq. (2), E_o stands for the total electron energy, E stands for the excitation energy of multipolarity λL and m is the electron rest energy.

The electrodisintegration cross section is very sensitive to the multipole composition of the photonuclear cross section. The experiment that will be discussed in this paper refers to the (e,2n) cross section in ^{181}Ta, in the energy region from threshold (14.2 MeV) to 22 MeV. In this energy region, besides the dominant E1 giant resonance, there are also the isoscalar E3 at $110A^{-1/3}$ MeV (19.5 MeV for ^{181}Ta) and the isovector E2 at $130A^{-1/3}$ (23 MeV for ^{181}Ta). Fig. 11 shows E1, E2 and E3 DWBA virtual photon spectra[7] for 20 MeV electrons scattered by a ^{181}Ta nucleus.

The isovector E2 and isoscalar E3 photonuclear sums are[8]:

$$S^{E2} = \int \sigma^{E2}(E)\, E^{-2}\, dE \simeq 0.22\, NZA^{-1/3}\ \mu b/MeV$$

$$S^{E3} = \int \sigma^{E3}(E)\, E^{-4}\, dE = 0.31\, Z^2\, A^{1/3}\ pb/MeV^3$$

yielding the values $S^{E2} = 306.6\ \mu b/MeV$ and $S^{E3} = 9.3 \mu b/MeV^3$ for ^{181}Ta. The corresponding integrated photonuclear cross sections are approximately:

$$A^{E2} \cong (23\ MeV)^2 \times S^{E2} = 162\ MeV.mb$$

$$A^{E3} \cong (19.5\ MeV)^4 \times S^{E3} = 1.3\ MeV.mb.$$

while the integrated $(\gamma,2n)$ cross section, using Saclay data is 881 MeV.mb[4]. Eventhough the E2 and E3 virtual photon spectra are more intense than the E1 spectra, one isovector E2 sum and/or one E3 isoscalar sum, all in the $(\gamma,2n)$ channel, have neglegible contribution to the (e,2n) cross section in ^{181}Ta, for the energy range considered here.

Thus, for the (e,2n) cross section in ^{181}Ta, eq. (2) reduces to:

$$\sigma_{e,2n}(E_o) = \int_o^{E_o-m} \sigma_{\gamma,2n}(E)\, N^{E1}(E_o,E,Z)\, \frac{dE}{E} \qquad (3)$$

It has been shown[8], in a precise test of the E1 virtual photon calculations, that electro and photodisintegration can be accurately related through Eq. (3).

Our measured $\sigma_{e,2n}$ cross section can, in principle, differ from the calculated cross section (right hand side of Eq. (3)) by a constant factor, due to a difference between our absolute scale and that of the $(\gamma,2n)$ data. This can be easily overcome by measuring also the photodisintegration yield produced when a radiator is placed in the electron beam ahead of the target. In such a measurement, one obtains:

$$\sigma_{br,x}(E_o) = N_r \int_o^{E_o-m} \sigma_{\gamma,x}(E)\, K(E_o,E,Z_r)\, \frac{dE}{E} \qquad (4)$$

where, N_r is the number of nuclei/cm^2 in the radiator of atomic number Z_r and $K(E_o,E,Z_r)$ is the bremsstrahlung cross section.

In the test of the El virtual photon spectrum[8] already mentioned, it was found that if the DBM bremsstrahlung cross section[10] is used in Eq. (4), electro and photo-disintegration are compatible within the experimental errors (~ 2%).

Thus, measuring $\sigma_{br,x}(E_o)$ and computing the ratio:

$$K = \left[\sigma_{br,x}(E_o)\right] / \left[N_r \int_o^{E_o - m} \sigma_{\gamma,x}(E)\ K(E_o,E,Z_r)\frac{dE}{E}\right] \qquad (5)$$

the constant K can be determined. This constant is the difference between the absolute scale of the $\sigma_{\gamma,x}$ measurement and that of the $\sigma_{e,x}$ and $\sigma_{br,x}$ measurements, since both were measured under the same experimental conditions.

4. THE EXPERIMENT

The $\sigma_{e,Tn}$ cross section ($\sigma_{e,Tn} = \sigma_{e,n} + 2\sigma_{e,2n}$) of ^{181}Ta was measured by counting the neutrons. The neutron detector system consists of four $^{10}BF_3$ counters embedded in paraffin. The efficiency of the detector was determined by measuring the (e,n) cross section in ^{63}Cu and comparing with the absolute measurements of ^{63}Cu(e,n) performed at the National Bureau of Standards[11]. The results obtained for $\sigma_{e,Tn}$ are shown in

Fig. 12 by the open circles.

The ^{181}Ta (e,n) cross section was measured by residual activity, following the 93.3 KeV γ-ray line that results from the decay of ^{180}Ta to ^{180}Hf. The results obtained for the (e,n) cross section are shown in Fig. 12 by the triangles.

The ^{181}Ta (e,2n) cross section can be easily obtained from the data of Fig. 12:

$$\sigma_{e,2n}(E_o) = \left[\sigma_{e,Tn}(E_o) - \sigma_{e,n}(E_o)\right]/2 \qquad (6)$$

and is shown in this same figure by the squares.

In order to determine the difference between our absolute scale and that of Saclay and Livermore, $\sigma_{br,n}(E_o)$ was measured for E_o = 24.5, 27.5 and 30.5 MeV, using a 0.329g/cm^2 copper radiator. With this measurement we determined K^S and K^L, using in Eq. (5) the (γ,n) cross section from Saclay and Livermore, respectively. The values obtained are:

$$K^S = 0.94 \pm 0.03$$
$$K^L = 1.29 \pm 0.04$$

The large difference between K^S and K^L results from the fact that the integrated (γ,n) cross sections from Livermore and Saclay are, respectively, 1300 MeV.mb and 2180 MeV.mb.

RESULTS AND DISCUSSION

In order to compare our $\sigma_{e,2n}$ cross section with

the Saclay and Livermore (γ,2n) results, we have to use in Eq. (3) the (γ,2n) cross section from Saclay multiplied by K^S and the (γ,2n) cross section from Livermore multiplied by K^L. The predicted cross sections are shown by the solid lines S and L in Fig. 12. At E_o = 22.5 MeV the calculated (e,2n) cross section using Livermore data is 63% higher than that obtained with the Saclay data. Our results are in good agreement with the (e,2n) cross section calculated using the Livermore (γ,2n) cross section and excludes the result obtained using the Saclay data.

Since $(\sigma^S_{\gamma,Tn}/\sigma^L_{\gamma,Tn})$ = 1.22 and our absolute scale requires the Livermore data to be multiplied by 1.29 ± 0.04, this implies that our absolute scale is compatible with the Saclay absolute scale. The value obtained for K^S is a consequence of the excess (γ,n) cross section above the (γ,2n) threshold. If we correct the Saclay (γ,n) cross section using:

$$\sigma^{S*}_{\gamma,n} = \sigma^S_{\gamma,Tn} - 2\sigma^{S*}_{\gamma,2n} \qquad (7)$$

the obtained $\sigma^{S*}_{\gamma,n}$ coincides with 1.22 x $\sigma^L_{\gamma,n}$. If we use $\sigma^{S*}_{\gamma,n}$ in Eq. 5, we obtain K^{S*} = 1.06 ± 0.04.

The conclusion is that our absolute measurement is in agreement with the Saclay absolute measurement for $\sigma_{\gamma,Tn}$, but our $\sigma_{e,2n}$ cross section shows that the neutron multiplicity sorting carried out by Livermore is correct. Since the branching of (γ,n) and (γ,2n) cross sections from Livermore is correct, the decay of the E1 Giant Resonance is statistical.

As mentioned previously, Saclay interpreted their

excess (γ,n) cross section as caused by fast neutrons and obtained that in heavy nuclei the direct effect was about 15%[1]. There are measurements of photoneutron spectra emitted from the E1 Giant Resonance which also yielded to the conclusion that the direct contribution in heavy nuclei was ~ 15%[12] suporting the Saclay results. These measurements of photoneutron spectra were compared with the results of a statistical calculation assuming that the levels of the residual nucleus are well described by a level density function:

$$\rho = \rho_o \exp(U/T) \qquad (8)$$

where U is the excitation energy and T is the temperature of the nucleus. The results of the statistical calculation were compared with the observed photoneutron spectra and the excess neutrons were interpreted as arising from direct emission.

It has been shown recently[13] that Eq. (8) is inadequate to describe the energy levels of the residual nucleus in the range of excitation energies covered by the E1 Giant Resonance. Dias and Wolynec[13] have shown that for the E0 Giant Resonance in ^{208}Pb, if Eq. (8) is used to represent the energy levels of ^{207}Pb, one would obtain 15% of direct contribution from the measured photoneutron spectra. However, if instead of using Eq. (8), the measured levels of ^{207}Pb are used, the decay of the E0 Giant Resonance by neutrons can be completely explained on a statistical basis. Dias and Wolynec pointed out that the conclusions derived from comparing photoneutron spectra from the E1 Giant Resonance with a

statistical calculation using Eq. (8) to describe the energy levels are questionable. All these photoneutron spectra have to be reanalized, using the actual levels of the corresponding residual nuclei, instead of Eq. (8).

As an example, H. Dias[14] has carried out the calculations described in ref. 12. for the E1 giant Resonance in ^{208}Pb. Figs. 13 and 14 show the measured photoneutron spectrum [12,15] and the result of a Hauser-Feshbach calculation using the energy levels of ^{207}Pb instead of Eq. (8). The agreement between the measured and predicted spectra shows that for ^{208}Pb the decay of the E1 Giant Resonance is statistical. Consequently,the fact that the Livermore results for (γ,n) and $(\gamma,2n)$ cross sections imply that the decay of the E1 Giant Resonance in medium and heavy nuclei is dominantly statistical is not in contradiction with other experimental evidences.

More recently Saclay has performed several measurements of total photoabsorption in nuclei, $\sigma_{\gamma,abs}$, using the fact that in heavy nuclei

$$\sigma_{\gamma,abs} \equiv \sum_x \sigma_{\gamma,xn}$$

since the Coulomb barrier inhibits charged particle emission. Neutron multiplicities up to ~ 10 are involved in such measurements. The Saclay error in the neutron multiplicity analysis observed in the separation of (γ,n) and $(\gamma,2n)$ events can, in principle,

become far more important for higher multiplicities.

As we have already pointed out, when the difference between Saclay and Livermore absolute scales is removed, the same patern is observed in all nuclei measured by both Laboratories: the (γ,n) cross sections from both Laboratories coincide up to the $(\gamma,2n)$ threshold. Above the $(\gamma,2n)$ threshold the (γ,n) cross sections from Saclay are always bigger than the corresponding Livermore cross sections. The $(\gamma,2n)$ cross sections from Saclay are always smaller than the corresponding Livermore cross sections. The same behaviour is observed in the recent total photoneutron measurements from Saclay. As an example, Saclay has measured for natural Zr the $\sigma^{(j)}$ cross sections[16]:

$$\sigma^{(j)} = \sum_{i=j}^{i_{max}} \sigma(\gamma,in) \qquad (9)$$

where i_{max} is the maximum photoneutron multiplicity measured. $\sigma^{(1)}$ is, then, the total photoneutron cross section. Fig. 15[16] shows $\sigma^{(1)}$ from Saclay (data points), for natural Zr, compared with the Livermore measurement (solid line). Both measurements coincide up to the lowest $(\gamma,2n)$ threshold (14.95 MeV for ^{94}Zr) and above this energy the Saclay cross section is bigger. Fig. 16[16] shows the Saclay $\sigma^{(2)}$ cross section (data points) compared with the Livermore cross section (solid line). The Saclay $\sigma^{(2)}$ cross section is smaller than the Livermore cross section. Note that below 23.6 MeV $\sigma^{(2)}$ should coincide with $\sigma_{\gamma,2n}$ from

Livermore (23.6 MeV is the $(\gamma,3n)$ threshold for ^{94}Zr).

CONCLUSIONS

The differences between the Saclay and Livermore photoneutron cross sections arise from the analysis that separates the total neutron counts in partial cross sections (neutron multiplicity sorting).

Our measurement of the (e,2n) cross section in ^{181}Ta shows that the neutron multiplicity sorting from Livermore is correct. There are two important consequences from that:

a) There are no large percentages of direct neutrons emitted from the El Giant Resonance. The decay of the El Giant Resonance is dominantly statistical.

b) The error in the Saclay neutron multiplicity sorting could affect seriously their more recent results for total photoabsorption.

ACKNOWLEDGMENTS

The authors acknowledge the financial support from Fundação de Amparo a Pesquisa do Estado de São Paulo, Financiadora de Estudos e Projetos and Conselho Nacional do Desenvolvimento Científico e Tecnológico. The authors also want to thank Dr. H. Dias for the statistical calculations of photoneutron spectra.

FIGURE CAPTIONS

Fig. 1 - $\sigma_{\gamma,Tn} = \sigma_{\gamma,n} + 2\sigma_{\gamma,2n}$ from Saclay (solid line) and Livermore (data points).

Fig. 2 - $\sigma^{S}_{\gamma,Tn}$ from Saclay divided by $\sigma^{L}_{\gamma,Tn}$ from Livermore. The Saclay and Livermore data were interpolated in order to have both cross sections at the same photon energies. The solid line shows R, the value obtained by fitting a constant to the ratio. R = 1.30 ± 0.02

Fig. 3 - The same as Fig. 2 but with the Livermore data displaced by - 410 KeV. R = 1.22 ± 0.02.

Fig. 4 - The same as Fig. 1 but with the Livermore data multiplied by 1.22 and displaced by -410 KeV.

Fig. 5 - $\sigma_{\gamma,n}$ from Livermore (data points) and Saclay (solid line). The Livermore data is displaced by -410 KeV and multiplied by 1.22.

Fig. 6 - $\sigma_{\gamma,2n}$ from Livermore (data points) and Saclay (solid line). The Livermore data is displaced by -410 KeV and multiplied by 1.22.

Fig. 7 - $\sigma_{\gamma,2n}$ from Livermore (data points) multiplied by 1.22 and displaced by -410 KeV. The solid line is the

modified $\sigma_{\gamma,2n}$ from Saclay:

$$\sigma^{S*}_{\gamma,2n} = \sigma^{S}_{\gamma,2n} + (1/2)(\sigma^{S}_{\gamma,n} - R\sigma^{L}_{\gamma,n})$$

Fig. 8 - The same as Fig. 5 but without displacement of the Livermore energy scale and R = 1.30.

Fig. 9 - The same as Fig. 6 but without displacement of the Livermore energy scale and R = 1.30.

Fig. 10 - The same as Fig. 7 but without displacement of the Livermore energy scale and R = 1.30.

Fig. 11 - DWBA E1, E2 and E3 virtual photon spectra for 20 MeV electrons inelastically scattered by a tantalum nucleus.

Fig. 12 - Measured $\sigma_{e,Tn}$ (circles), $\sigma_{e,n}$ (triangles) and $\sigma_{e,2n}$ (squares) versus the electron incident energy. The solid lines show the predicted $\sigma_{e,2n}$ cross sections using Saclay and Livermore data for $\sigma_{\gamma,2n}$.

Fig. 13 - Spectrum of photoneutrons from the E1 giant resonance in ^{208}Pb. The data points are from ref. 12. The solid line is the result of a Hauser-Feshbach calculation using the energy levels of ^{207}Pb.

Fig. 14 - Spectrum of photoneutrons from the E1 giant resonance in ^{208}Pb (ref. 15). The solid line is the

result of a Hauser-Feshbach calculation using the energy levels of ^{207}Pb.

Fig. 15 - $\sigma^{(1)}$ from Saclay (data points) and Livermore (solid line) for natural Zr (ref. 16).

Fig. 16 - $\sigma^{(2)}$ from Saclay (data points) and Livermore (solid line) for natural Zr (ref. 16).

REFERENCES

1. E. Wolynec, A.R.V. Martinez, P. Gouffon, Y. Miyao, V.A. Serrão, and M.N. Martins, Phys. Rev. C29, 1137 (1984).

2. R. Bergère, H. Beil, and A. Veyssiere, Nucl. Phys. A121, 463 (1968).

3. R.L. Bramblet, J.T. Caldwell, G.P. Auchampaugh, and S.C. Fultz, Phys. Rev. 129, 2723 (1963).

4. Atlas of Photoneutron Cross Sections Obtained with Monoenergetic Photons, Bicentennial Edition, Preprint UCRL-78482, Edited by B. L. Berman.

5. B.L. Berman and S.C Fultz, Rev. Mod. Phys. 47, 713 (1975).

6. H. Beil, R. Bergère, and A. Veyssiere, Nucl. Instr. and Meth. 67, 293 (1969).

7. W.W. Gargaro and D.S. Onley, Phys. Rev. C4, 1032 (1971) and C. W. Soto Vargas, D.S. Onley, and L.E. Wright, Nucl. Phys. A288, 45 (1977).

8. W.R. Dodge, E. Hayward, and E. Wolynec, Phys. Rev. C28, 150 (1983).

9. E. Hayward, in Giant Multipole Resonances, edited by Fred E. Bertrand (Harwood Academic, New York, 1980).

10. J.L. Mathews and R.O. Owens, Nucl. Instr. and Meth. 111, 157 (1973).

11. M.N. Martins, E. Hayward, G. Lamaze, X.K. Maruyama, F. Schima, and E. Wolynec, scheduled for publication in the december issue of Phys. Rev. C.

12. J.R. Calarco, Ph. D. Thesis, University of Illinois (1968) and S.S. Hanna, in Giant Multipole Resonances, edited by Fred E. Bertrand (Harwood Academic, New York, 1980).

13. H. Dias and E. Wolynec, Phys. Rev. C (Scheduled for publication in october).

14. H. Dias, private communication.

15. M.E. Toms and W.E. Stephens, Phys. Rev. 108, 77 (1957).

16. A. Veyssiere, H. Beil, R. Bergère, P. Carlos, J. Pagot, A. Leprete, and A. Miniac, Z. Phys. A306, 139 (1982).

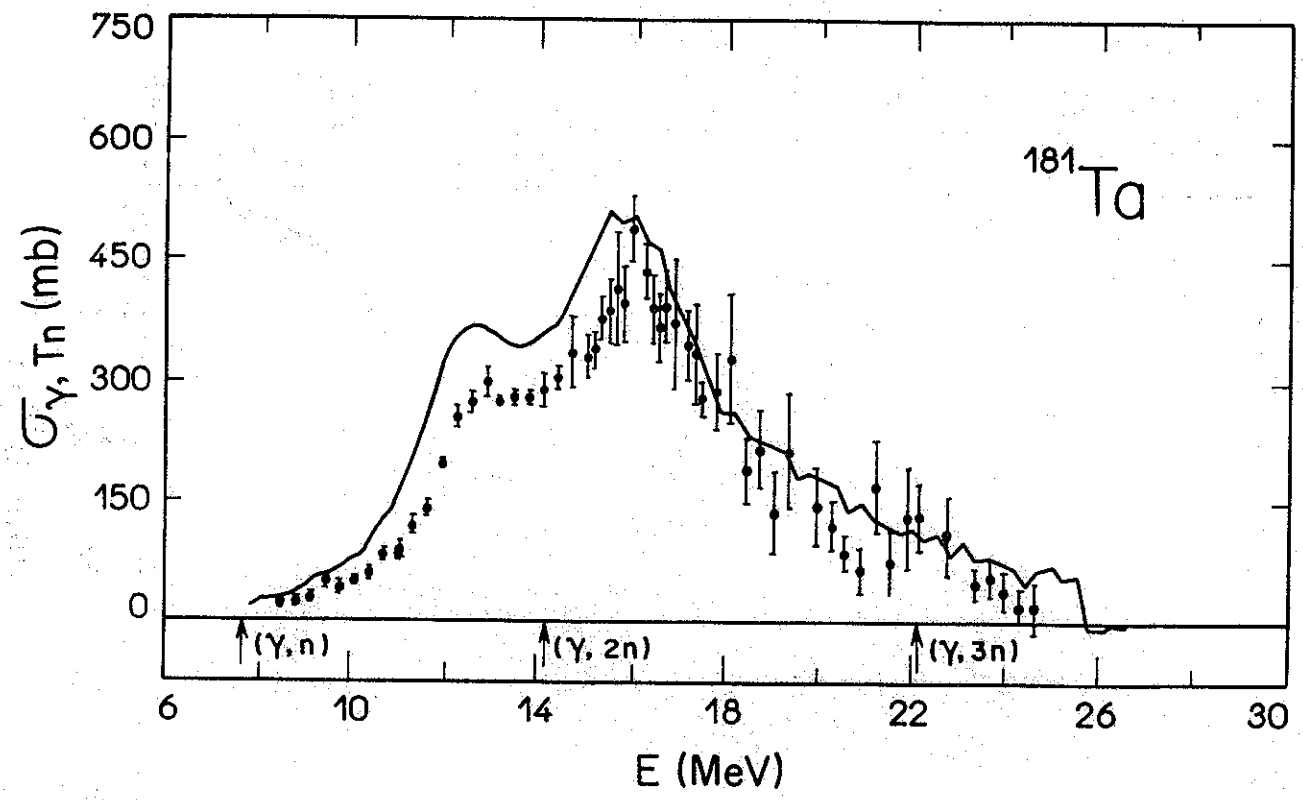
750
600
450
300
150
0
$\sigma_{\gamma,Tn}$ (mb)
^{181}Ta
(γ, n)
(γ, 2n)
(γ, 3n)
6
10
14
18
22
26
30
E (MeV)

Fig. 1

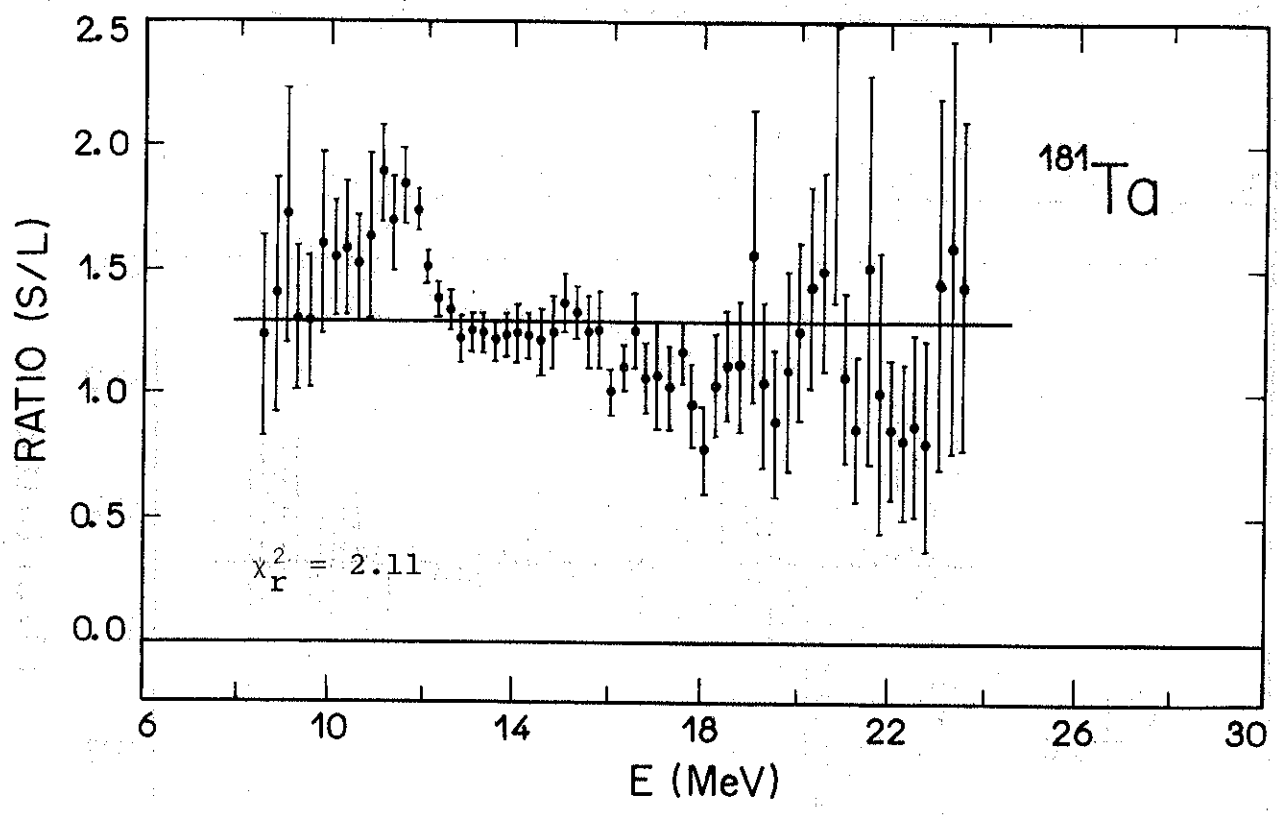
2.5
2.0
1.5
1.0
0.5
0.0
RATIO (S/L)
^{181}Ta
χ^2_r = 2.11
6
10
14
18
22
26
30
E (MeV)

Fig. 2

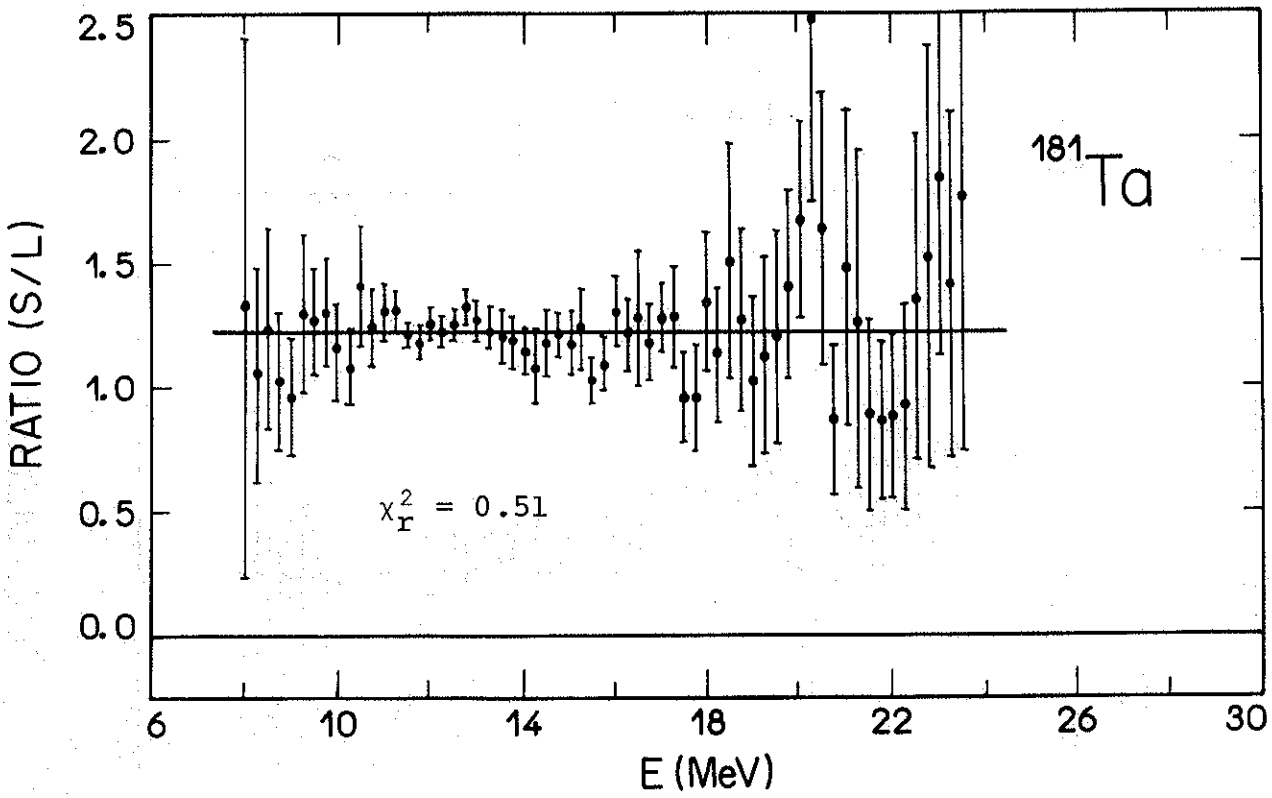
RATIO (S/L)
E (MeV)
^{181}Ta
χ^2_r = 0.51

Fig. 3

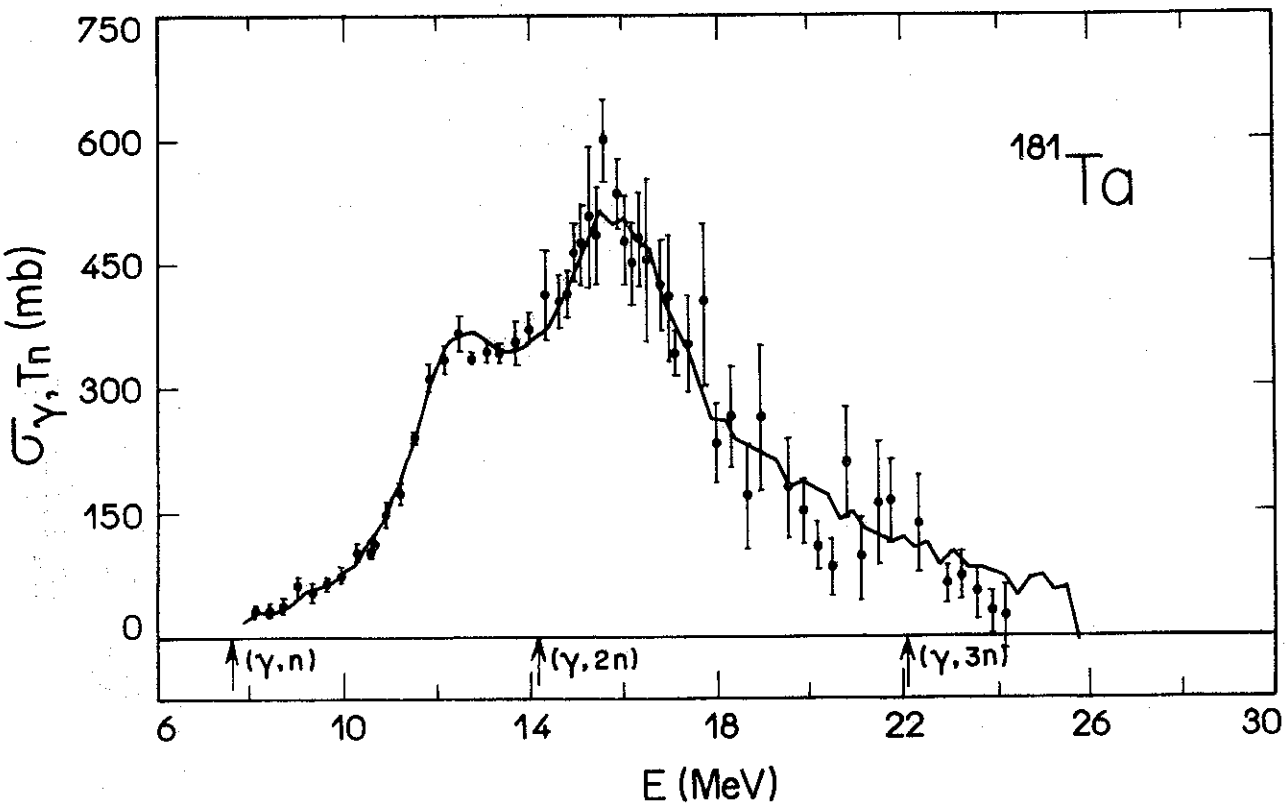
$\sigma_{\gamma,Tn}$ (mb)
E (MeV)
^{181}Ta
(γ,n)
(γ,2n)
(γ,3n)

Fig. 4

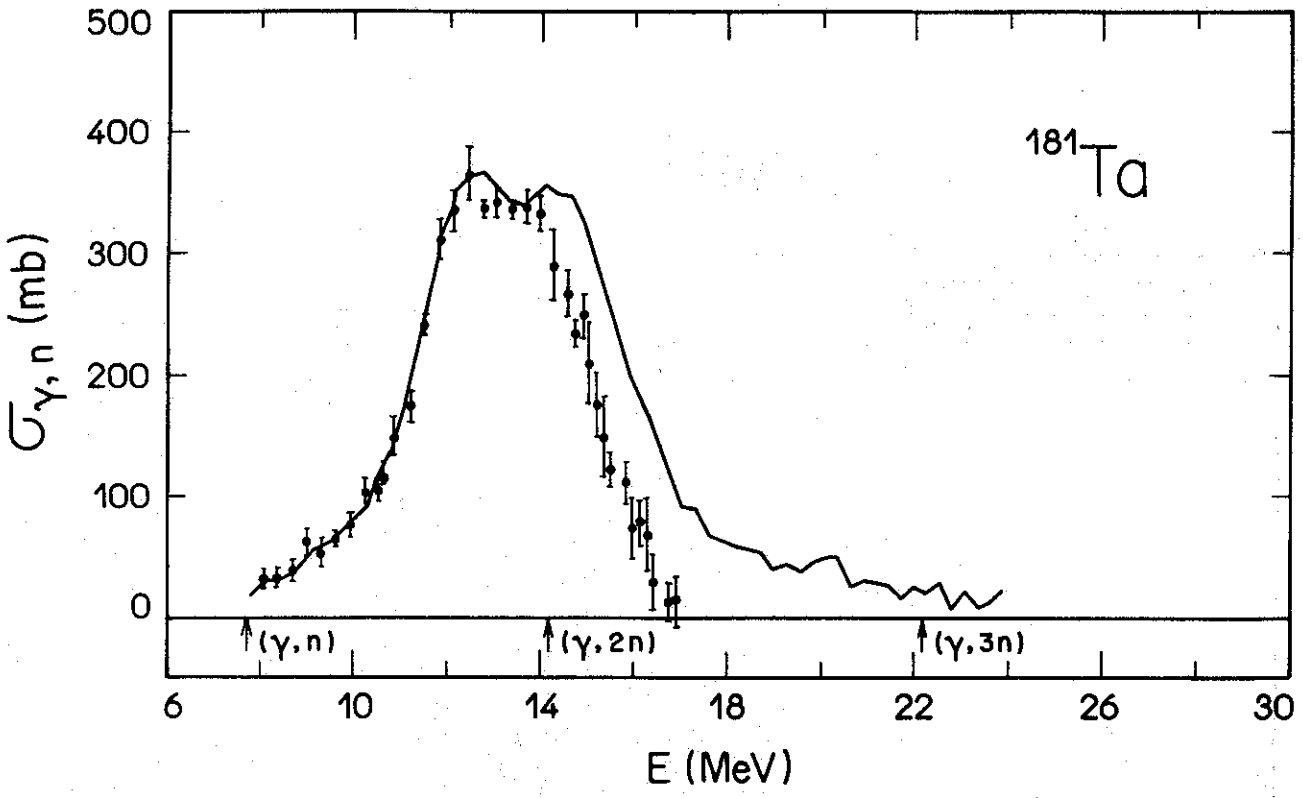
500
400
300
200
100
0
$\sigma_{\gamma,n}$ (mb)
^{181}Ta
(γ,n)
(γ,2n)
(γ,3n)
6
10
14
18
22
26
30
E (MeV)

Fig. 5

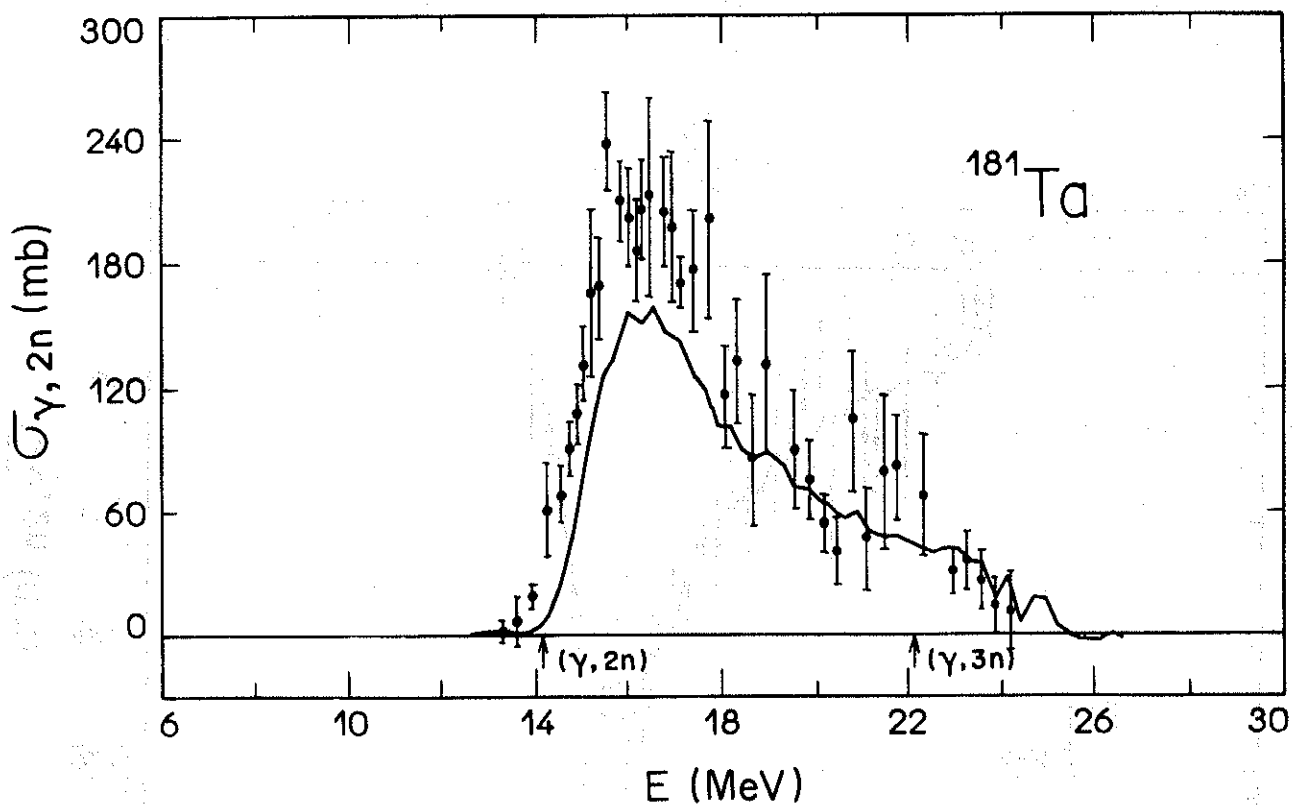
300
240
180
120
60
0
$\sigma_{\gamma,2n}$ (mb)
^{181}Ta
(γ,2n)
(γ,3n)
6
10
14
18
22
26
30
E (MeV)

Fig. 6

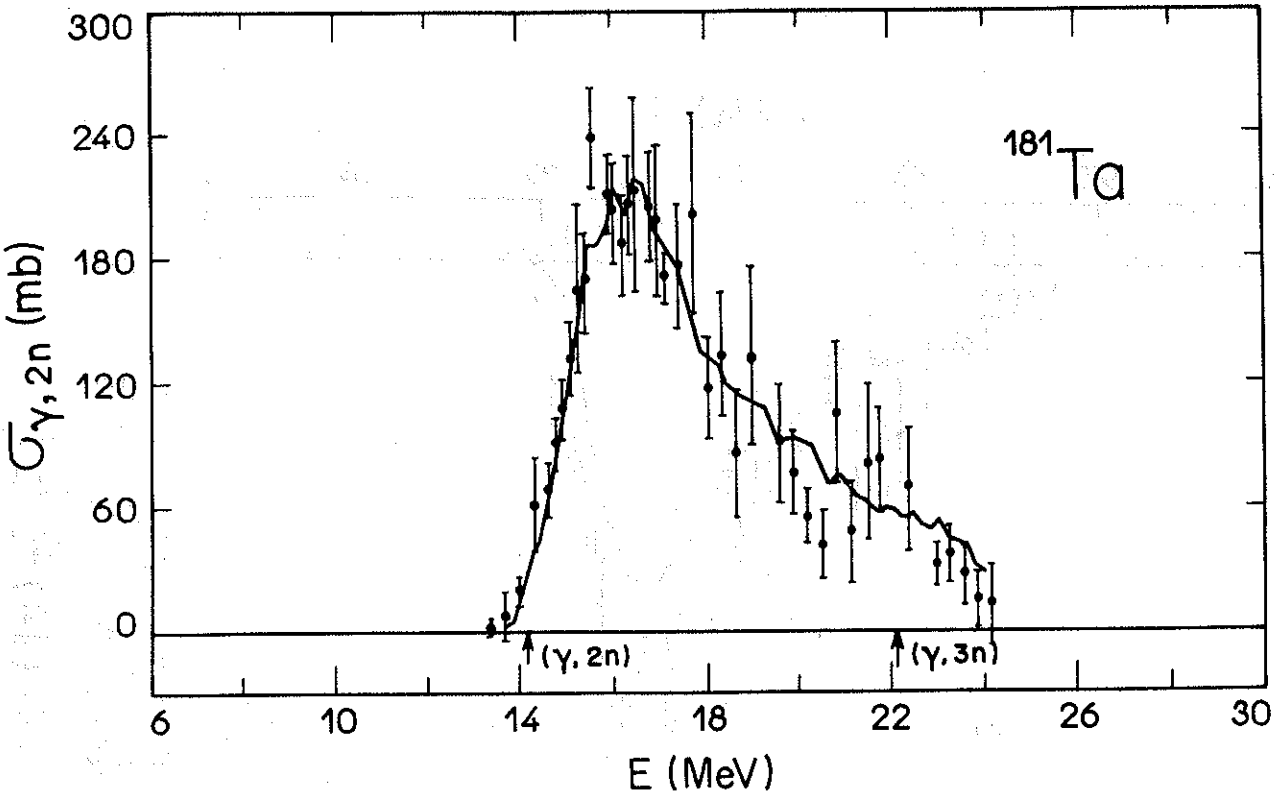
300
240
180
120
60
0
$\sigma_{\gamma,2n}$ (mb)
^{181}Ta
(γ, 2n)
(γ, 3n)
6
10
14
18
22
26
30
E (MeV)

Fig. 7

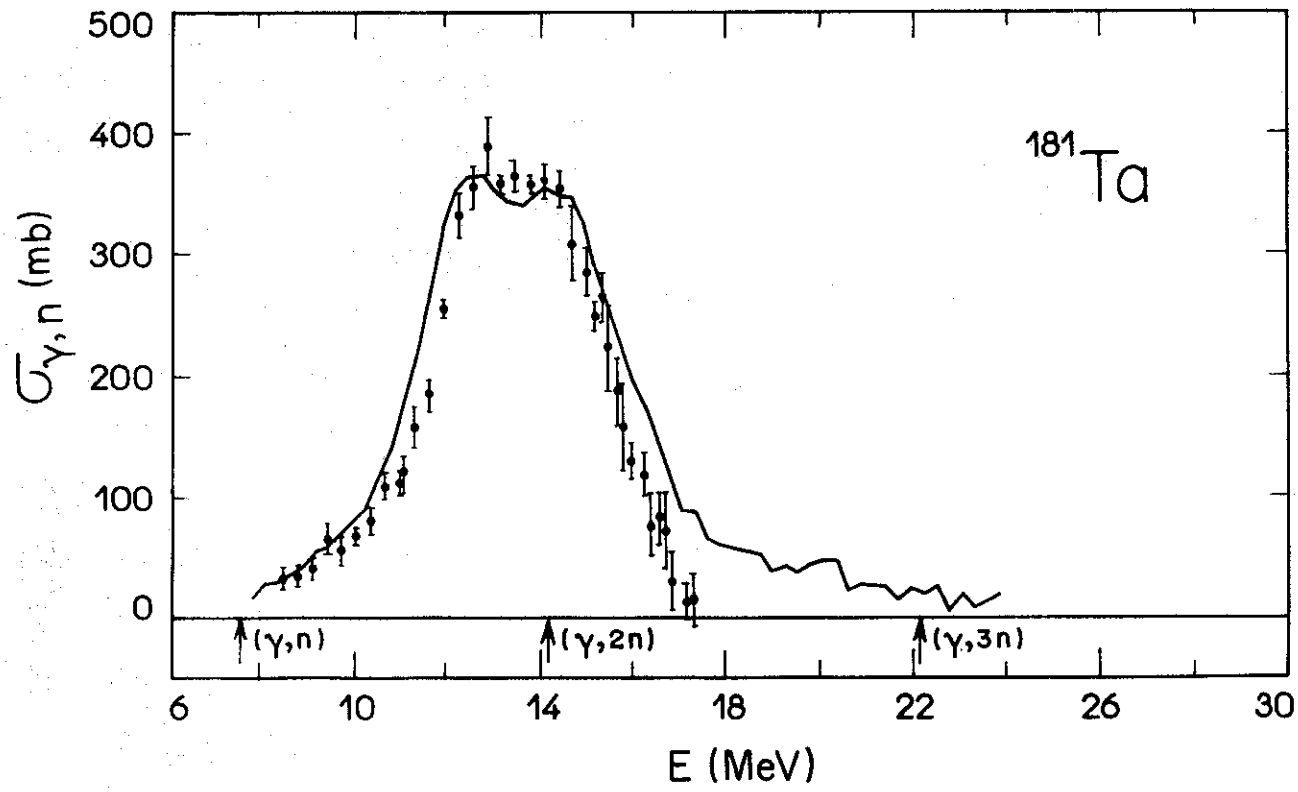
500
400
300
200
100
0
$\sigma_{\gamma,n}$ (mb)
^{181}Ta
(γ,n)
(γ,2n)
(γ,3n)
6
10
14
18
22
26
30
E (MeV)

Fig. 8

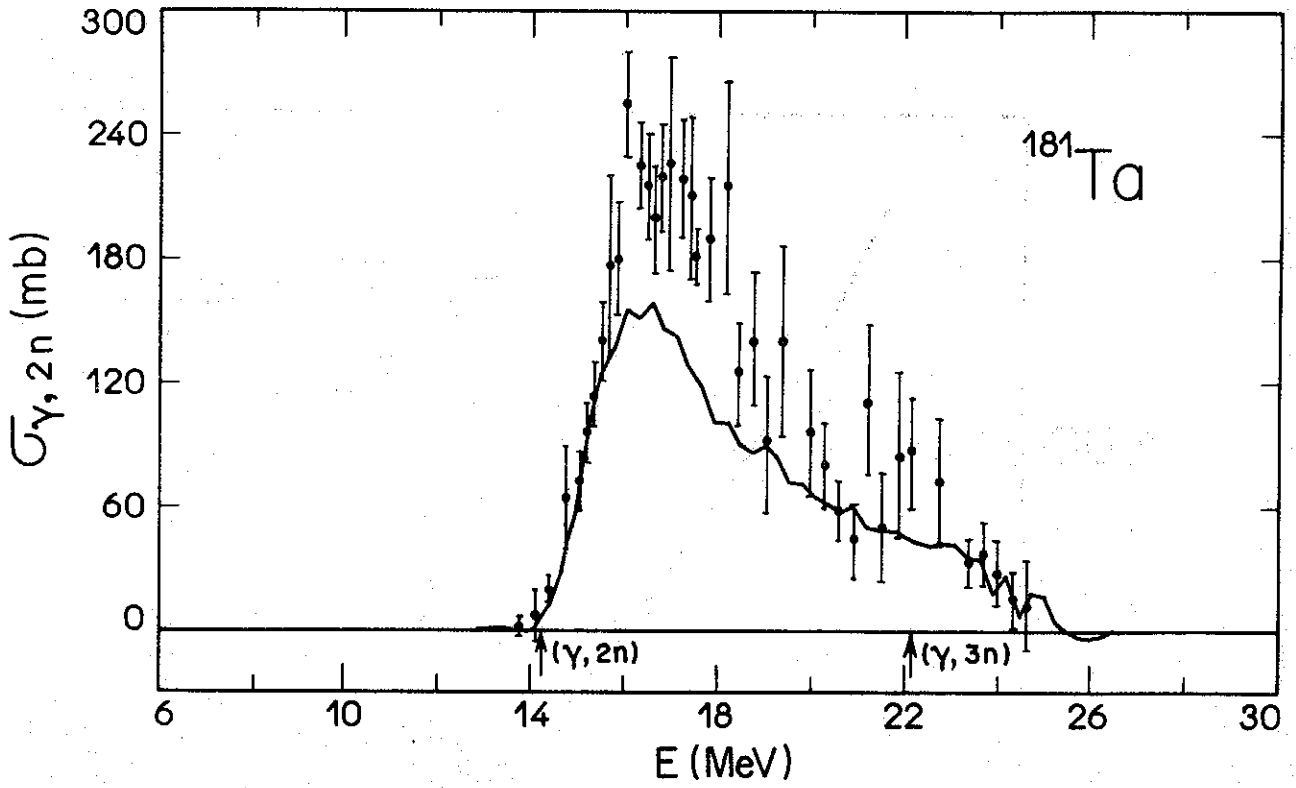
300
240
180
120
60
0
$\sigma_{\gamma,2n}$ (mb)
^{181}Ta
(γ, 2n)
(γ, 3n)
6
10
14
18
22
26
30
E (MeV)

Fig. 9

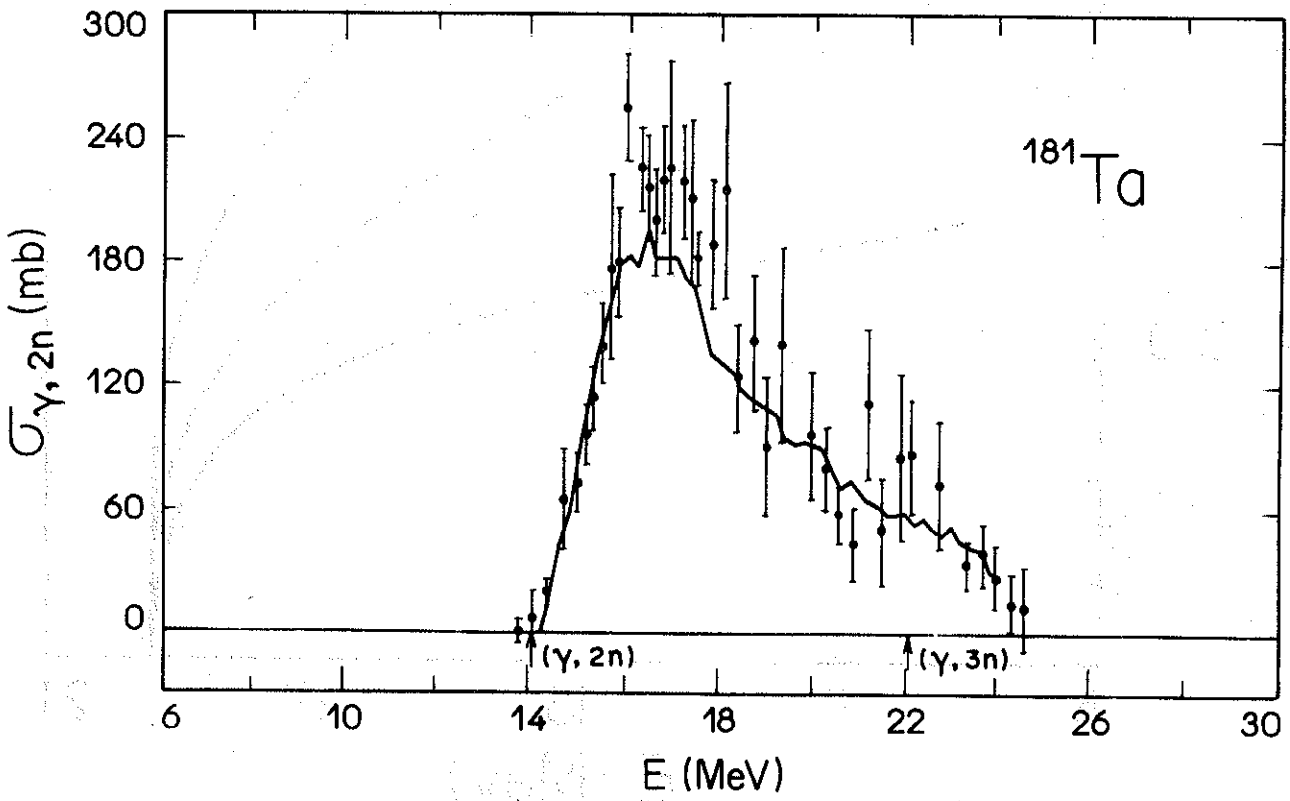
300
240
180
120
60
0
$\sigma_{\gamma,2n}$ (mb)
^{181}Ta
(γ, 2n)
(γ, 3n)
6
10
14
18
22
26
30
E (MeV)

Fig. 10

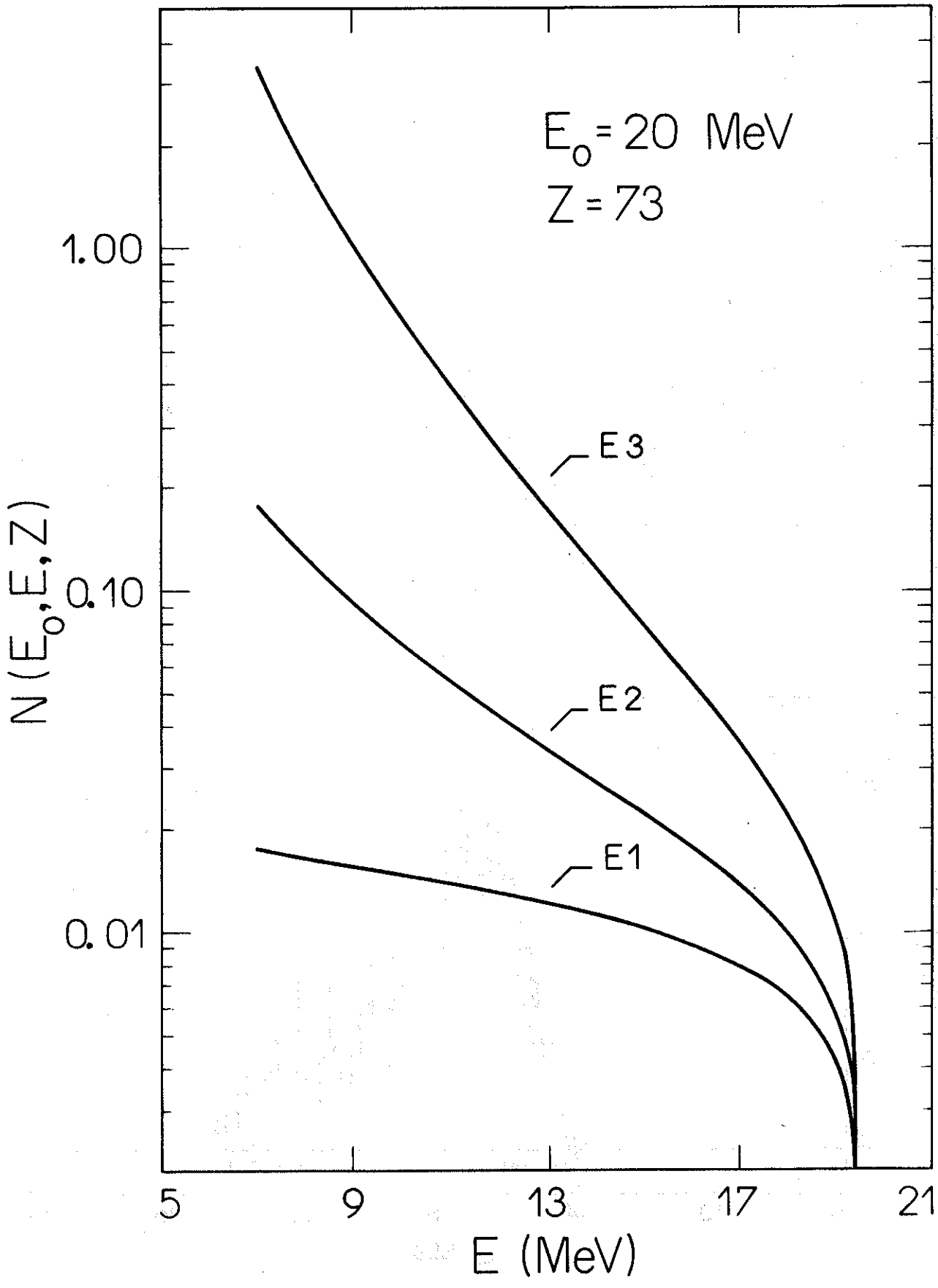

Fig. 11

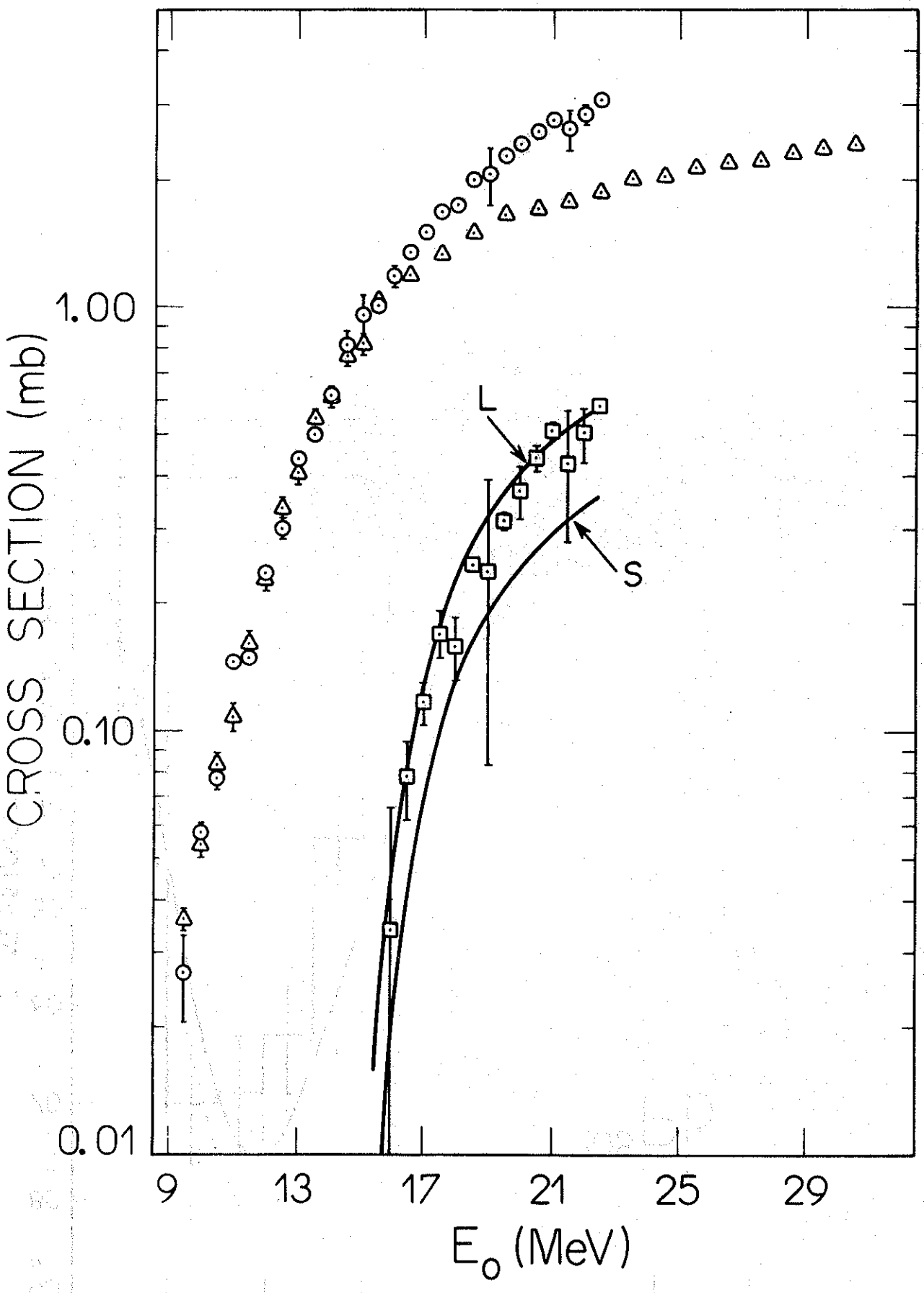

Fig. 12

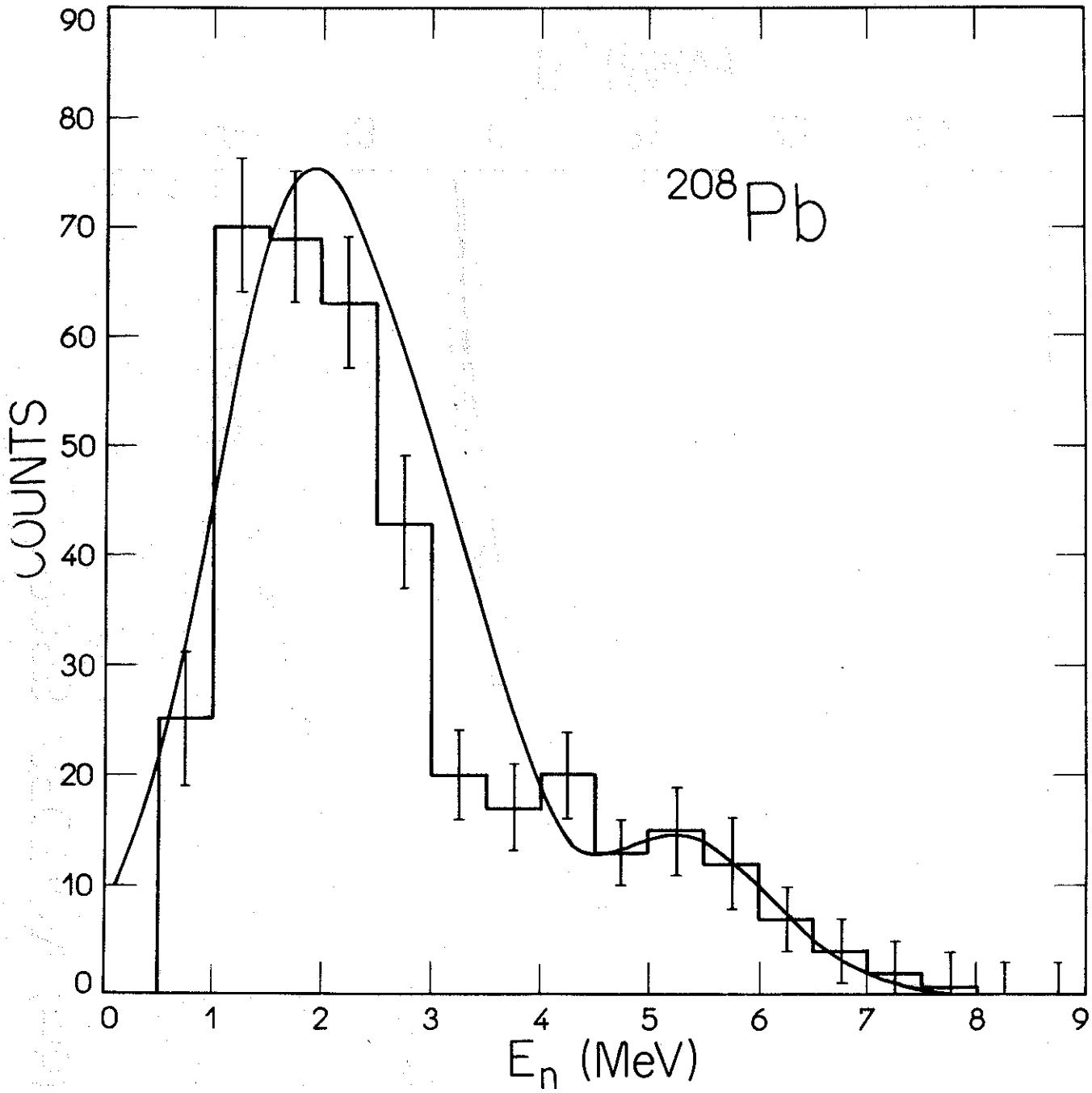

Fig. 13

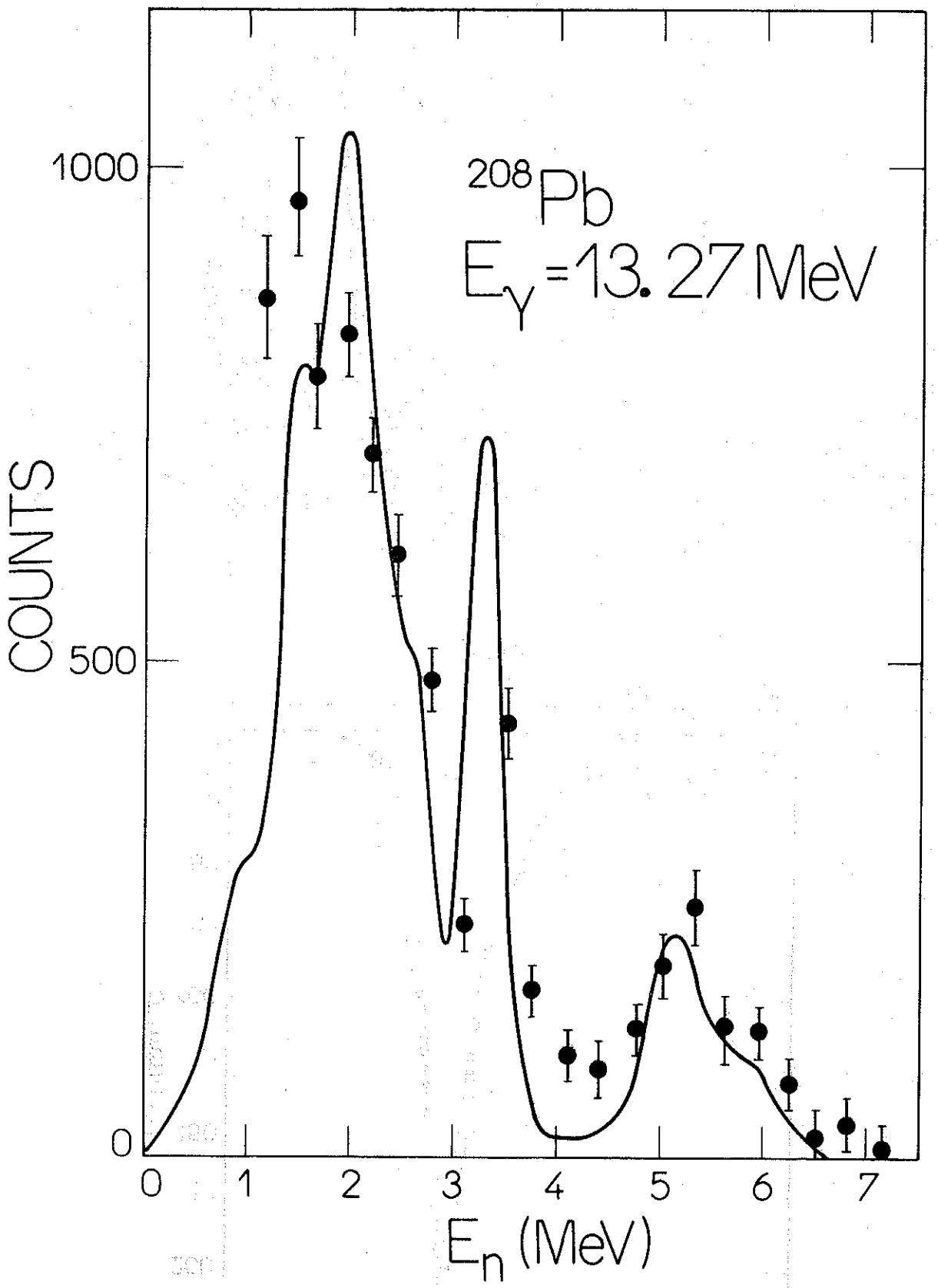

Fig. 14

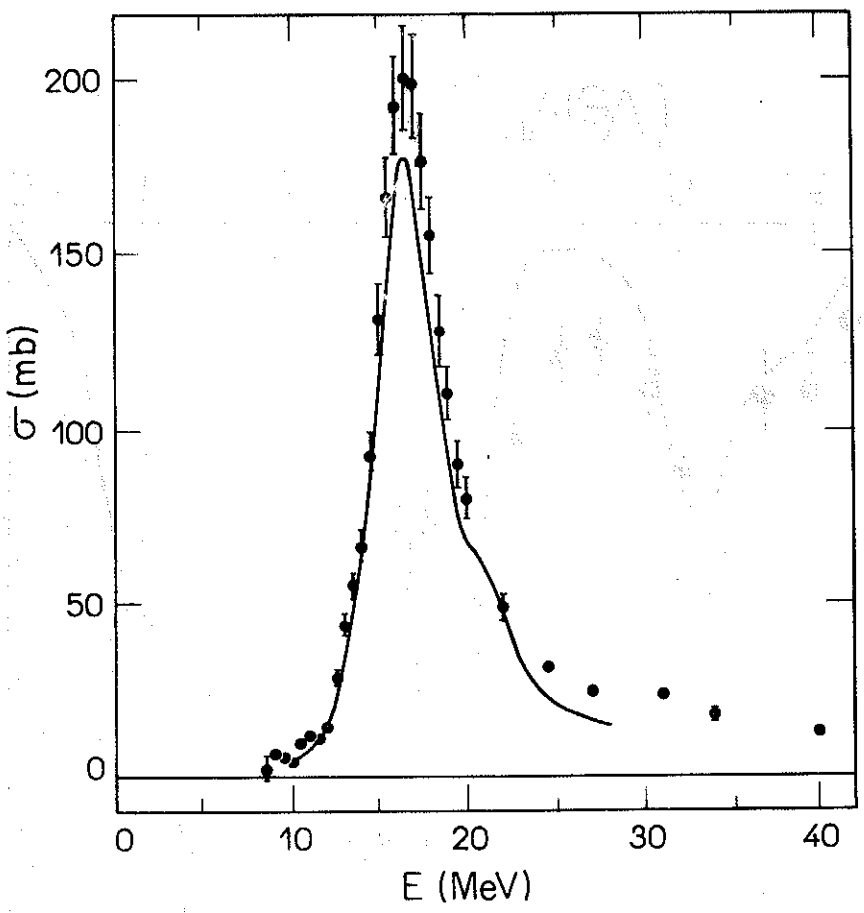
200
150
100
50
0
σ (mb)
0
10
20
30
40
E (MeV)

Fig. 15

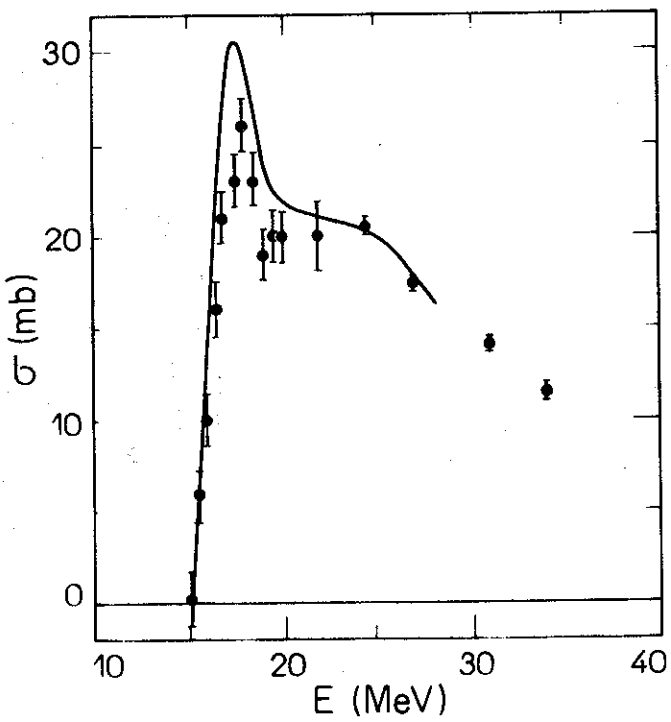
30
20
10
0
σ (mb)
10
20
30
40
E (MeV)

Fig. 16